JOURNAL OF CATALYSIS 116, 230–239 (1989)

Propane Hydrogenolysis over Supported Nickel Catalysts: Structural and Support Effects

P. A. BURKE AND E. I. KO[1]

Department of Chemical Engineering, Carnegie Mellon University, Pittsburgh, Pennsylvania 15213

Received June 24, 1988; revised October 4, 1988

Kinetic data for propane hydrogenolysis were determined for Ni catalysts supported on SiO_2, Nb_2O_5, Nb_2O_5–SiO_2, and TiO_2. Over a metal particle size range of 2.5–6.0 nm, the activities for three Ni/SiO_2 catalysts varied by no more than a factor of 5. The lowest activity was found for a sample which had been reduced under the most severe conditions and believed to have a large proportion of (111) planes. The sample with the smallest particle size showed a higher selectivity. Activities for Ni supported on the other three oxides were lower, indicative of support effects. For samples reduced at 773 K, the suppression in activity varied in the order $Nb_2O_5 > TiO_2 \sim Nb_2O_5$–$SiO_2$. The metal–support interactions were reversible by oxidizing the samples and rereducing at a lower temperature. An oxygen treatment at 473 K was sufficient to recover the activity of Ni/TiO_2 but not for Ni/Nb_2O_5, which required an oxygen treatment at 673 K. A model which considers the overall energetics of the regeneration process is presented to explain this difference.

1. INTRODUCTION

The concept of structural sensitivity is relatively clear-cut for reactions occurring on single crystal surfaces but less so for supported metal catalysts. A structure-sensitive reaction is usually defined as one whose rate (measured as turnover frequency) varies with particle size (*1*). Such an operational definition has certain pitfalls. First, it is important to vary the particle size in an appropriate range over which a significant change in surface structure is expected to occur. Second, particle size as a parameter may be insufficient to characterize surface structure. Our work with Ni/SiO_2 catalysts (*2, 3*), for example, showed that two catalysts with similar particle sizes can indeed have different surface structures influenced by preparation method and pretreatment conditions.

The rate of a structure-sensitive reaction can also be affected by support effects. This situation is particularly true for the so-called SMSI catalysts (*4*). It has been firmly established that, for these systems, one important aspect of the interaction involves the migration of the supporting oxide over the metal particles (*5*). Such a "decoration" suppresses the activity for the hydrogenolysis of paraffins, as has been reported by many investigators (*6*).

In an attempt to quantify the relative importance of structural and support effects on a structure-sensitive reaction, we have studied the hydrogenolysis of propane over a series of Ni catalysts supported on SiO_2 and three interacting oxides. As shown in Table 1, this reaction has been widely used as a chemical probe for Ni catalysts (*7–12*). In this paper, we report activity and selectivity data which will shed light on the surface structure of Ni particles and the driving force for oxide migration in SMSI systems.

2. EXPERIMENTAL

2.1. Sample Preparation

All the supported Ni catalysts used in this study are summarized in Table 2; their

[1] To whom correspondence should be addressed.

0021-9517/89 $3.00

TABLE 1

Summary of Literature Results of Propane Hydrogenolysis over Nickel

Reference	Catalyst	Preparation method[a]	Reduction temperature [K]/time [h]	Particle diameter [nm]	Temperature[b] [K]	Pressure [Torr][b]		Activity[c] $\times 10^4$ [s^{-1}]		
						Propane	Hydrogen	r_1	r_2	r_3
7	Evaporated nickel film	—	—	—	490–540	3.7	44.5	—	—	27
8	Ni/Al_2O_3: E′	CP	773/16	12	473–623	24–95	143–380	—	—	9.2
	F′	CP	773/16	20				—	—	0.07
9	Ni/SiO_2	I	723/24–40	3	527–576	190	1140	—	—	21
10	Ni/SiO_2	—[d]	873/-	3.5	523	50	150	—	—	429
11	Ni/SiO_2	P	950/15	6	483–573	2–25	100–600	112	246	358
12	Ni/SiO_2: A	P	920/15	6.4	465–580	1–63	63–760	40	66	106
	B	P	1200/15	21	507	25	160	3.1	5.5	8.6

[a] Preparation method: CP, coprecipitation; I, impregnation; P, precipitation.

[b] Temperature and pressure are summarized over either a given range or at the value which was reported.

[c] Activity calculated for T = 500 K, $P_{propane}$ = 22.8 Torr, $P_{hydrogen}$ = 152 Torr. Whenever available, activities for the hydrogenolysis to ethane (r_1) and to methane (r_2) are included in addition to total activity (r_T).

[d] Pentane solution of $Ni(\pi\text{-}C_3H_5)_2$.

preparation and characterization are described in detail elsewhere (*13–16*). Briefly, the silica-supported nickel catalysts with a range of crystallite sizes from 2.5 to 6 nm were prepared either by the incipient wetness impregnation of nickel nitrate hexahydrate or by a precipitation method using nickel nitrate hexammine solution (*13*). The catalysts were then dried overnight at 353 K in stagnant air and stored in a desiccator until use. The niobia–silica surface phase oxide support, NS(I), was prepared by the incipient wetness impregnation of silica (Davison 952) with a solution of niobium

TABLE 2

Characteristics of Supported Nickel Catalysts

Support	Notation	Preparation method[a]	Weight[b] % Ni	Reduction temperature [K]/time [h]	Percentage reduction[c]	Ni particle size[d] [nm]
SiO_2:	A-18	I	18	773/4	100	5.5
	Cl-20	P	20	1050/15	100	6.0
	C-20	P	20	773/4	70	2.5
NS(I):	NS(I)-573	I	10	573/1	30	3.0
	NS(I)-773	I	10	773/1	100	5.5
Nb_2O_5:	Nb-573	I	10	573/1	100	4.0
	Nb-773	I	10	773/1	100	4.0
	Nb-773-R473-573	I	10	773/1-O_2[e] 473/2-573/1	100	4.0
	Nb-773-R673-573	I	10	773/1-O_2[e] 673/2-573/1	100	3.5
TiO_2:	Ti-573	I	10	573/1	42	12
	Ti-773	I	10	773/1	100	12
	Ti-773-R473-573	I	10	773/1-O_2[e] 473/2-573/1	86	15
	Ti-773-R673-573	I	10	773/1-O_2[e] 673/2-573/1	34	14

[a] Preparation method: I, impregnation; P, precipitation.

[b] Determined by initial loading and confirmed by atomic absorption spectroscopy.

[c] Percentage of nickel reduced determined by thermogravimetric analysis (*14*).

[d] Ni particle size determined by X-ray diffraction line broadening for all catalysts. Results for Ni/SiO_2 are confirmed by hydrogen chemisorption and magnetic measurements (*2, 3*).

[e] These samples were reduced in H_2 at 773 K for 1 h, oxidized in O_2 at the temperature shown for 2 h, and rereduced in H_2 at 573 K for 1 h.

(V)ethoxide (Alpha Products) and hexane to achieve monolayer coverage. The impregnated sample was dried in a vacuum overnight to remove the solvent and then calcined at 773 K for 2 h in oxygen after a 2-h pretreatment in nitrogen at 673 K. Bulk niobia and titania supports were prepared in a manner similar to that described by Tauster and Fung (*17*). The procedure consisted of titrating a methanolic solution of niobium(V)chloride or titanium(IV)chloride with ammonium hydroxide to a pH of 7. The resultant precipitate was filtered and washed repeatedly until no chloride ions were detectable by precipitation of silver nitrate in the filtrate. The precipitate was then dried overnight at 373 K in stagnant air and calcined as outlined above. The resultant bulk niobia, titania, and NS(I) supports were TT-niobia, anatase, and amorphous, respectively, as found by X-ray diffraction (XRD). Their corresponding BET surface areas were measured with a commercial Quantasorb unit to be 70, 100, and 267 m^2/g. Nickel catalysts on the interacting supports were prepared by incipient wetness impregnation of nickel nitrate hexahydrate, dried overnight at 373 K, and stored in a desiccator until use. Prior to kinetic studies, the supported nickel catalysts were reduced in flowing H_2 at 50 cc/min for different times and temperatures as shown in Table 2. For convenience the samples and pretreatments will be referred to following the notations in Table 2.

2.2. Kinetic Study

Experiments were carried out using the same apparatus and procedures described earlier for ethane hydrogenolysis (*18*). Briefly, a stainless-steel microreactor was operated in a differential mode at one atmosphere pressure with on-line gas chromatography for product analysis. The total flowrate was held constant at 18 liter/min with helium (Airco 99.999%) used as a diluent. Propane (Airco 99.98%) and hydrogen (Airco 99.999%) partial pressures were varied from 15.2 to 76 and from 76 to 228 Torr, respectively. Propane, helium, and hydrogen were further purified over 4A (Linde) molecular sieve and hydrogen and helium were also purified over oxygen absorption units (Engelhard and Matheson, respectively).

The hydrogenolysis of propane proceeds by two pathways:

$$C_3H_8 + H_2 \rightarrow C_2H_6 + CH_4 \quad (1)$$

$$C_3H_8 + 2H_2 \rightarrow 3CH_4 \quad (2)$$

We refer to these pathways as reaction 1 and reaction 2 in this paper. Since ethane is less reactive than propane, its further hydrogenolysis to methane is negligible at low conversions. For each pathway, an experimental rate law can be established in the form

$$r_i = k_i \exp\left[-\frac{E_{ai}}{RT}\right] P_{H_2}^{m_i} P_{C_3H_8}^{n_i},$$

where r_i is the turnover frequency, E_{ai} is the apparent activation energy, and m_i and n_i are the reaction orders with respect to hydrogen and propane, respectively, for reaction i.

Turnover frequencies were calculated from the weight loading, percentage reduction, and particle size of each sample shown in Table 2. A "bracketing" procedure similar to that used by Yates *et al.* (*19*) was used in measuring the exponents n and m. The loss of activity was slight over a typical series of runs. Blank runs also showed that there was no background activity under our experimental conditions.

3. RESULTS

3.1. Silica-Supported Ni

Table 3 summarizes the kinetic parameters for the three Ni/SiO_2 catalysts. All three samples showed nearly identical apparent activation energies and reaction orders with respect to hydrogen and propane. The Cl-20 sample, however, is less active than the other two by about a factor of 4. Figure 1 shows that this difference is well beyond the scatter of experimental data.

TABLE 3

Propane Hydrogenolysis over Ni/SiO_2[a]

Catalyst	Activity $\times 10^4$ [s^{-1}]		E_{a1}	E_{a2}	P_{H_2}		$P_{C_3H_8}$	
			[kcal/mole]					
	r_1	r_2			m_1	m_2	n_1	n_2
A-18	14.3	11.9	39	64	−1.6	−3.0	1.0	1.0
C-20	18.7	9.7	36	57	−1.8	−3.3	0.9	0.9
Cl-20	3.4	2.8	36	61	−1.6	−2.8	0.9	0.9

[a] Kinetic parameters for the rate law $r_i = k_i \exp(-E_{ai}/RT)P_{H_2}^{m_i}P_{C_3H_8}^{n_i}$. Subscripts 1 and 2 denote reaction 1 and 2, respectively. Experimental conditions were: T = 478 K, P_{H_2} = 152 Torr, and $P_{C_3H_8}$ = 22.8 Torr.

Note also the nearly identical activities of the two other samples.

Figure 2 shows a plot of the log of selectivity, defined as (r_1/r_2), as a function of reciprocal temperature. The A-18 and Cl-20 samples have almost identical selectivities despite differences in activities. The selectivity for the C-20 sample was higher.

3.2. *Nickel Supported on Interacting Oxides*

Results of propane hydrogenolysis over Ni supported on Nb_2O_5, Nb_2O_5–SiO_2, and TiO_2 are summarized in Table 4 and Figs. 3 and 4. In the figures only the endpoints of the fitted lines are shown for clarity. The actual scatter of data was similar to that shown in Fig. 1. For the purpose of com-

TABLE 4

Propane Hydrogenolysis for Ni Supported on Interacting Oxides[a]

Catalyst	Activity $\times 10^4$ [s^{-1}]		E_{a1}	E_{a2}	P_{H_2}		$P_{C_3H_8}$	
			[kcal/mole]					
	r_1	r_2			m_1	m_2	n_1	n_2
A-18	86	232	39	64	−1.6	−3.0	1.0	1.0
NS(I)-573	76	122	36	63	−1.4	−2.7	0.8	0.9
NS(I)-773	13	26	34	58	−1.3	−2.4	1.0	0.9
Nb-573	1.6	2.8	32	47	−1.1	−2.0	0.9	0.9
Nb-773	0.25	0.14	14	34	−0.1	−0.7	0.9	0.6
Nb-773-R473-573	0.45	0.22	19	39	−0.3	−0.8	0.9	0.6
Nb-773-R673-573	1.9	2.5	34	50	−1.5	−2.6	0.8	0.8
Ti-573	12	25	39	57	−1.1	−2.0	0.9	0.9
Ti-773	3.7	8.3	34	50	−1.1	−2.0	0.8	1.0
Ti-773-R473-573	20	40	38	54	−1.3	−2.2	0.9	0.8
Ti-773-R673-573	19	36	37	51	−1.0	−1.9	0.9	0.8

[a] Kinetic parameters for the rate law $r_i = k_i \exp(-E_{ai}/RT)P_{H_2}^{m_i}P_{C_3H_8}^{n_i}$. Subscripts 1 and 2 denote reaction 1 and 2, respectively. Experimental conditions were: T = 500 K, P_{H_2} = 152 Torr, and $P_{C_3H_8}$ = 22.8 Torr.

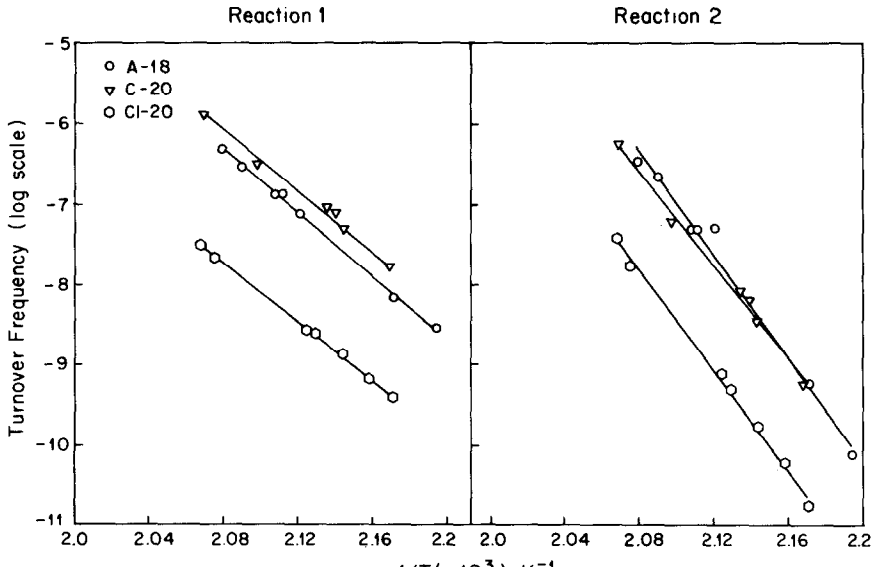

FIG. 1. Arrhenius plots of the two reaction pathways of propane hydrogenolysis over Ni/SiO_2 catalysts.

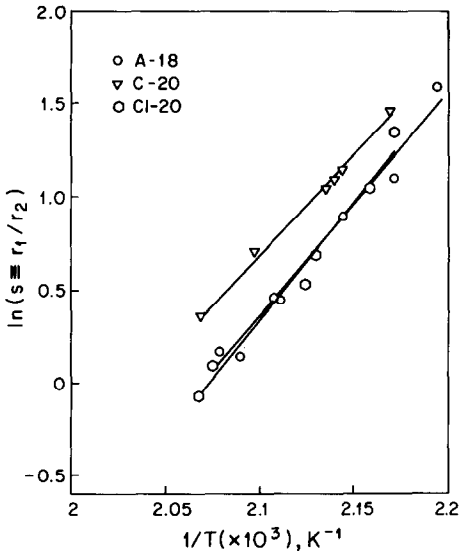

FIG. 2. Selectivity of the three Ni/SiO_2 catalysts for propane hydrogenolysis plotted as a function of $\ln(r_1/r_2)$ versus reciprocal temperature.

parison the results for A-18 are included to be representative of a noninteracting system. After reduction at 573 K, the lowest temperature used in this study, the activity of Ni/Nb_2O_5 was less than that of Ni/SiO_2, and the extent of suppression became more severe at the higher reduction temperature of 773 K. The loss in activity (close to a factor of 10^3) is well beyond the range which is spanned by the three Ni/SiO_2 catalysts (see Table 3). A support effect is thus firmly established, as previously done for ethane hydrogenolysis (*18*). Using the activity as a gauge, we further observe that Nb_2O_5–SiO_2 and TiO_2 were less interactive than Nb_2O_5 under similar conditions, an observation which is also in accord with earlier reports (*16, 18*).

3.3. Regeneration

One interesting and important feature of a SMSI catalyst is that its chemisorptive and catalytic properties can be reverted by an oxidation treatment followed by a low temperature reduction. In order to determine whether the regenerative behavior differs between oxides, we attempted to restore the hydrogenolysis activity for Ni supported on bulk Nb_2O_5 and TiO_2. Our procedure was to first reduce the catalyst at 773 K for 1 h, then oxidize in pure O_2 at a

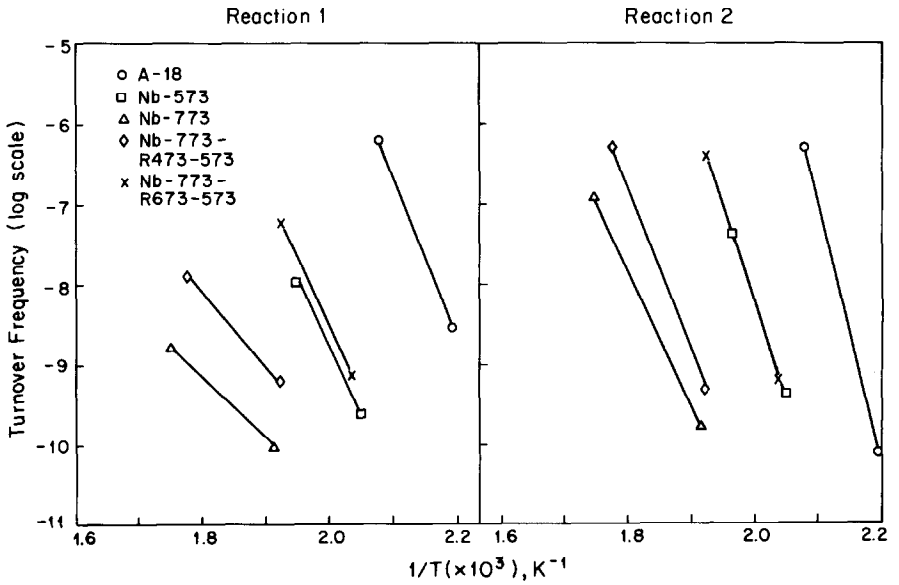

FIG. 3. Activity of propane hydrogenolysis for Ni supported on Nb_2O_5. Results for sample A-18 are included for comparison.

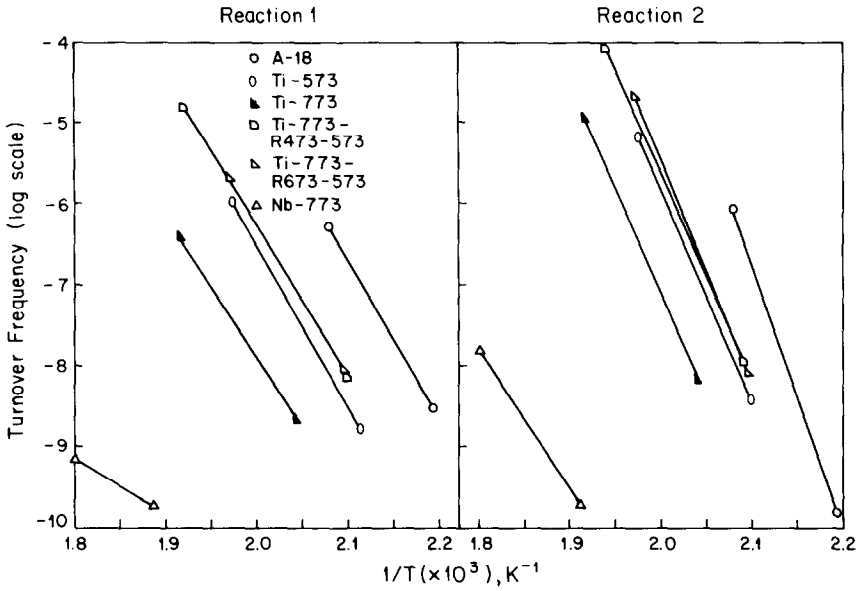

FIG. 4. Activities of propane hydrogenolysis for Ni supported on TiO_2. Results for sample A-18 and Nb-773 are included for comparison.

specific temperature for 2 h, and rereduce at 573 K for 1 h. The activity was measured after the second reduction treatment.

Table 4 and Fig. 3 show that for Ni/Nb_2O_5, when the oxidation step was at 473 K, the activity increased somewhat but was lower than the sample originally reduced at 573 K. However, an oxidative treatment at 673 K completely restored the kinetic parameters not only in activity, but also in activation energy and reaction order.

Another evidence of the regenerability of Ni/Nb_2O_5 comes from the selectivity data. Figure 5 shows that the Nb-773 sample had the highest selectivity. The Nb-773-R473-573 sample, despite a small increase in activity, showed no change in selectivity. Only after an oxidative treatment at 673 K did the selectivity resemble that of the Nb-573 sample.

Table 4 and Fig. 4 show that Ni/TiO_2 catalysts can also be regenerated by the oxidation–reduction recycle. One important difference, though, is that total regeneration (in terms of restoration in activity) was achieved in this system after oxygen treatments at both 473 and 673 K. In other words, a milder condition was sufficient to "destroy" SMSI.

4. DISCUSSION

4.1. Structural Effects

The nearly identical activation energies and reaction orders (Table 3) found for propane hydrogenolysis over the three Ni/SiO_2 catalysts suggest that SiO_2 is indeed a noninteracting support. There are, however, differences in activity and selectivity. Compare first the data for A-18 and Cl-20, the average particle sizes of which were found previously to be similar by hydrogen chemisorption and X-ray diffraction line broadening (*2*). Still, the A-18 sample was more active by a factor of 4. This observation cannot be explained by preparation method alone (impregnation versus precipitation) since the C-20 sample was as active as A-18.

We believe the lower activity of Cl-20 was due to a larger portion of (111) surface planes on the nickel particles due to the

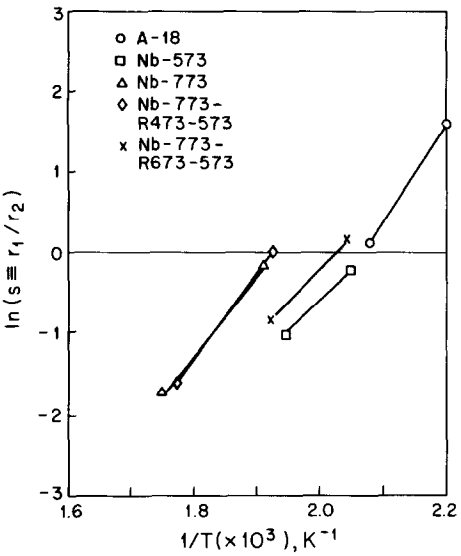

FIG. 5. Selectivity of Ni/Nb_2O_5 catalysts showing the effect of oxidation temperature on the regenerability.

more severe reduction treatment. Other authors (*12, 20*) have suggested that reduction at higher temperatures or longer times leads to the growth of Ni (111) planes. Goodman (*21*) reported that Ni (111) was less active than Ni (100) for ethane hydrogenolysis, and it is likely that the same is true for propane. Finally, our previous IR study of H_2/CO coadsorption over the same catalysts (*3*) showed that the A-18 sample does have a high ratio of (100) to (111) planes. It was found in the same study that the A-18 and C-20 samples have similar IR fingerprints, which would support their similar activities for propane hydrogenolysis. The important conclusion of these results is that distribution of surface planes, rather than average particle size, is the fundamental parameter with which activities among catalysts of different preparations and pretreatments should be compared.

Despite their difference in activity, the A-18 and Cl-20 samples have the same selectivity (Fig. 2). There are two possible explanations: either the (111) plane is equally less active for the two reaction pathways or the contribution from (100) planes dominates. Our data cannot differentiate these two possibilities. Another interesting observation is the higher selectivity of C-20. Again, our previous IR work (*3*) provides an explanation. Because of its small particle size, the C-20 sample does not have a large amount of extended smooth planes. It will thus be more difficult to find a large enough ensemble of nickel atoms to catalyze the second reaction (*12*).

Finally, it is worthwhile to compare our activity data to the literature results. In Table 1, literature data are calculated for our experimental conditions of $T = 500$ K, $P_{H_2} = 152$ Torr, and $P_{C_3H_8} = 22.8$ Torr. Even with the uncertainty usually associated with such an extrapolation, it is reassuring that an activity of $2–3 \times 10^{-2}$ s^{-1} for our A-18 and C-20 samples compares well with the literature range of $1–4 \times 10^{-2}$ s^{-1} for catalysts reduced under relatively mild conditions (*10–12*). Furthermore, lower activities have been reported in the literature for samples which are reduced at more severe conditions (*9, 12*). As discussed earlier, (111) planes are expected to be dominant in these samples, as on evaporated nickel film (*7*). The very low activity reported by Shephard (*8*) for Ni/Al_2O_3 is most likely due to a support effect similar to the one found by Taylor *et al.* (*19*) for ethane hydrogenolysis and possibly to the high temperature catalyst pretreatment in N_2 (1033–1433 K for 16 h).

4.2. *Support Effects*

Nickel catalysts on the Nb_2O_5, Nb_2O_5–SiO_2, and TiO_2 supports were all prepared by incipient wetness impregnation and had physical characteristics which are similar to A-18. The significantly lower activities they exhibited for propane hydrogenolysis were thus due to support effects, as previously observed for ethane hydrogenolysis (*16, 18, 22*). Part of the interaction is structural in nature, as it is now generally accepted that in these SMSI systems the surface of catalyst particle is decorated by a migrating

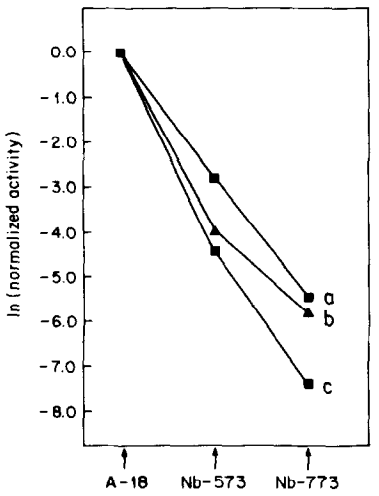

FIG. 6. Comparison of reaction rates over silica- and niobia-supported Ni catalysts for (a) ethane hydrogenolysis, (b) reaction 1, and (c) reaction 2 of propane hydrogenolysis.

oxide (*5*). The blocking of sites thus lowers the activity of structure-sensitive reactions such as the hydrogenolysis of paraffins (*1*). In a series of papers (*11, 12, 23*), Martin and co-workers showed that the ensemble size necessary for reaction increases from ethane hydrogenolysis to the reaction 1 and then to the reaction 2 of propane hydrogenolysis. One would thus anticipate the severity of a support effect due to site blocking to increase in the same direction. Such a trend is qualitatively established in Fig. 6, which shows the normalized rates of the three reactions on a Ni/Nb_2O_5 sample reduced at two temperatures. The more severely suppressed reaction 2 over reaction 1 for the Nb-773 sample also translates into a higher selectivity which is shown in Fig. 5.

Although the driving force for oxide migration in a SMSI catalyst is not completely understood at present, direct metal–cation bonding has been identified for some systems (*24–26*). If this is true, then the regeneration process must involve the breaking of such a bond. One can envision the regeneration step as

$$M\text{–}Y\text{–}O_x + O_2 \rightarrow M\text{–}O + O\text{–}Y\text{–}O_x,$$

where M denotes the metal and Y the cation. The overall energetics of this step is given by

$$E = \begin{pmatrix}\text{energy required in breaking}\\ \text{the } M\text{–}Y \text{ bond}\end{pmatrix} + \begin{pmatrix}\text{energy required in breaking}\\ \text{the O–O bond}\end{pmatrix} + \begin{pmatrix}\text{energy released from the}\\ \text{formation of the } M\text{–O bond}\end{pmatrix} + \begin{pmatrix}\text{energy released from the}\\ \text{formation of the O–}Y\text{ bond}\end{pmatrix}.$$

For comparison among different metal/support systems, only three of the four terms need to be considered since the energy in breaking the O–O bond remains constant. There are, however, other difficulties. The exact valence of the cation is not known and even if it is, there is no simple way to calculate the metal–cation bond energy. As an approximation, we treat the cation as a zero-valence species and estimate the relevant bond energies by using the method of Pauling (*27*). Briefly, the ionic and covalent contributions to the bond strength were calculated from data of electronegativities and heats of sublimation or literature bonding energies, respectively. Results thus obtained for several systems of interest are shown in Table 5.

Table 6 summarizes the energetics for various metal/support combinations. For

TABLE 5

Estimation of Bond Energies from Using Pauling's Method[a]

	Bond energy (kcal/mole)			
	O	Ti	V	Nb
O	33.2[b]	105.7	100.6	102.1
Ni	81.6	11.0	10.7	12.8
Rh	59.9	19.7	18.3	20.4
Ir	61.8	20.4	19.1	21.1
Pt	59.2	20.1	18.8	20.8

[a] See Ref. (*27*).
[b] Single-bond energy.

TABLE 6

Estimated Energetics for the Regeneration for Various SMSI Systems[a]

Metal	Support		
	TiO_2	V_2O_3	Nb_2O_5
Ni	−176.3	−171.5	−170.9
Rh	−145.9	−142.2	−141.6
Ir	−147.1	−143.3	−142.8
Pt	−144.8	−141.0	−140.5

[a] Calculated for the process $M - Y - O_x + O_2 \rightarrow M - O + O - Y - O_x$ with the omission of the energy for breaking the O–O bond. Values are reported in kilocalories per mole.

the two catalysts used in this study, the calculation shows that it would be more energetically favorable to regenerate Ni/TiO_2. Qualitatively, this can be understood in terms of the weaker Ti–Ni bond and stronger Ti–O bond compared to Nb. Experimentally we showed that oxidation at 473 K was sufficient to regenerate Ni/TiO_2 but not Ni/Nb_2O_5. When comparison is made for different metals on the same support, Table 6 suggests that Ni is the easiest to regenerate mainly because of the high Ni–O and weaker Ni–Y bond strengths. It has been reported (*28*) that Rh, Ir, and Pt do not fully regenerate even after an oxygen treatment at 503 K. Finally, the observation that Rh/TiO_2 regenerates more easily than Rh/V_2O_3 (*29*) is also in qualitative agreement with the relative energetics shown in Table 6.

Since our calculations do not include factors such as the different oxidizing properties of noble metals (*30*) and possible particle effects in oxidations (*31*), they are not expected to reveal subtle differences and peculiarities in some regeneration studies (*32, 33*). However, that such a crude model is consistent with the qualitative trend exhibited by the limited regeneration data available has important implications. First, it supports the notion of direct metal–cation bonding. The driving force for SMSI can be viewed as the reverse for regeneration. In our study, a stronger Ni–Nb bond makes Ni/Nb_2O_5 a more interacting system and one which is harder to regenerate. Second, regeneration studies have often been done simply as a check of SMSI behavior. Our results suggest that with the right chemical probe, extensive regeneration experiments may shed more light on these systems.

5. SUMMARY

The structure sensitivity of propane hydrogenolysis has been demonstrated from kinetic measurements over a series of supported Ni catalysts. For SiO_2-supported Ni, the activity is influenced by the type of planes exposed, with the (111) plane being less active than the (100). The relative amount of each plane is controlled by the pretreatment conditions and not necessarily related to the average particle size. However, with increasingly smaller particles, the concept of an extended smooth plane eventually breaks down. This will have a stronger effect on a reaction which requires a larger ensemble, resulting in a change in selectivity.

Support effects can result in more significant changes in activity and selectivity. For the supports used in this study, at least part of the effect is also structural in nature and involves site blocking over the catalyst particles. The interaction is reversible, however, and the ease of regeneration depends on a particular metal/support combination. A simple model which considers the relative energetics of different SMSI systems has been shown to be in qualitative agreement with experimental trends.

ACKNOWLEDGMENT

We acknowledge the support of this research by the Niobium Products Co., Inc.

REFERENCES

1. Boudart, M., and Djega-Mariadassou, G., "Kinetics of Heterogeneous Catalytic Reactions." Princeton Univ. Press, Princeton, NJ, 1984.

2. Blackmond, D. G., and Ko, E. I., *J. Catal.* **94,** 343 (1985).
3. Blackmond, D. G., and Ko, E. I., *J. Catal.* **96,** 210 (1985).
4. Tauster, S. J., Fung, S. C., and Garten, R. L. *J. Amer. Chem. Soc.* **100,** 170 (1978).
5. Tauster, S. J., *ACS Symp. Ser.* **298,** 1 (1986).
6. Stevenson, S. A., Raupp, G. B., Dumesic, J. A., Tauster, S. J., and Baker, R. T. K., "Metal–Support Interactions in Catalysis, Sintering, and Redispersion," Chap. 6. Van Nostrand–Reinhold, New York, 1987.
7. Anderson, J. P., and Baker, B. G., *Proc. Soc. London A* **271,** 402 (1963).
8. Shephard, F. E., *J. Catal.* **14,** 148 (1969).
9. Machiels, C. J., and Anderson, R. B., *J. Catal.* **58,** 253 (1979).
10. Ryndin, Y. A., Karpova, L. A., and Yemakov, Y. I., *React. Kinet. Catal. Lett.* **21,** 125 (1982).
11. Dalmon, J. A., and Martin, G. A., *J. Catal.* **66,** 214 (1980).
12. Guilleux, M. F., Dalmon, J. A., and Martin, G. A., *J. Catal.* **62,** 235 (1980).
13. Blackmond, D. G., and Ko, E. I., *Appl. Catal.* **13,** 49 (1984).
14. Ko, E. I., Hupp, J. H., Rogan, F. H., and Wagner, N. J., *J. Catal.* **84,** 85 (1983).
15. Chen, J. P., Ph.D. thesis, Carnegie Mellon University, 1986.
16. Ko, E. I., Bafrali, R., Nuhfer, N. T., and Wagner, N. J., *J. Catal.* **95,** 260 (1985).
17. Tauster, S. J., and Fung, S. C., *J. Catal.* **82,** 279 (1983).
18. Ko, E. I., Hupp, J. H., and Wagner, N. J., *J. Catal.* **86,** 315 (1984).
19. Yates, D. J. C., Taylor, W. F., and Sinfelt, J. H., *J. Amer. Chem. Soc.* **86,** 2996 (1964).
20. Yacaman, M. J., and Gomez, A., *Appl. Surf. Sci.* **19,** 348 (1984).
21. Goodman, D. W., *Surf. Sci.* **123,** L679 (1982).
22. Ko, E. I., and Garten, R. L., *J. Catal.* **68,** 233 (1981).
23. Martin, G. A., *J. Catal.* **60,** 345 (1979).
24. Sakellson, S., McMillian, M., and Haller, G. L., *J. Phys. Chem.* **90,** 1733 (1986).
25. Sadeghi, H. R., and Henrich, V. E., *J. Catal.* **109,** 1 (1988).
26. Haller, G. L., and Resasco, D. E., "Advances in Catalysis," in press.
27. Pauling, L., "The Nature of the Chemical Bond." Cornell Univ. Press, New York, 1960.
28. Meriandeau, P., Ellestad, O. H., Dufaux, M., and Naccache, C., *J. Catal.* **75,** 243 (1982).
29. Lin, Y., Resasco, D. E., and Haller, G. L., *J. Chem. Soc., Faraday Trans. 1* **83,** 2091 (1987).
30. Barr, T. L., *J. Phys. Chem.* **82,** 1801 (1978).
31. Betteridge, W., and Rhys, D. W., *Congr. Corrosion* **1,** 186 (1961).
32. Foger, K., *J. Catal.* **78,** 406 (1982).
33. Anderson, J. B. F., and Burch, R., *Appl. Catal.* **25,** 173 (1986).